# The Co-development of Offshore Wind and Hydrogen in the UK – A Case Study of Milford Haven South Wales

**Fulin Fan[1], John Nwobu[2,*], David Campos-Gaona[1]**

[1] Department of Electronic and Electrical Engineering, University of Strathclyde, G1 1XW Glasgow, United Kingdom
[2] Offshore Renewable Energy Catapult, G1 1RD Glasgow, United Kingdom

[*] E-mail: john.nwobu@ore.catapult.org.uk

**Abstract**. Green hydrogen produced from renewable energy resources can not only contribute to the decarbonisation of different energy sectors, but also serve as a carrier for long-distance delivery of renewable generation, offering a cost-effective way to exploit the renewables far from electrical grids. To facilitate the co-development of offshore wind and hydrogen, the paper develops a modelling framework to dispatch power and hydrogen flows across dedicated offshore wind hydrogen production systems to meet onshore hydrogen demands while keeping similar state of charge levels between multiple systems. Then the hydrogen supply to shore and the system investments and ongoing costs are discounted to their present values to calculate the levelised cost of hydrogen, which is minimised by the particle swarm optimsiation algorithm to suggest the best capacities of hydrogen system components including converters, desalination devices, electrolysers, compressors and storage assets. The proposed modelling framework is tested based on a case study at Milford Haven South Wales which is evaluated to have massive offshore wind resources in the Celtic Sea and comparable demands for hydrogen by 2040. The optimisation results are presented based on the techno-economic input parameters projected for 2030 and 2050 scenarios and discussed alongside the influences of technology advances on the system optimisation and resulting metrics including the levelised costs of hydrogen, net present values and potential levels of green hydrogen supply to Milford Haven.

## 1. Introduction

The global end of reliance on fossil fuels for power and efforts towards achieving a net zero economy are driving a clean energy revolution [1]. Conventional $CO_2$ producing energy processes are currently being replaced with carbon-free solutions presenting a promising growth area in the energy transition. Low carbon hydrogen is one of the main alternative energies powering the energy industry's transition and offers a huge potential for carbon free energy [2]. The UK has outlined a comprehensive roadmap for its low carbon hydrogen sector development in the 2020s [3] and doubled the hydrogen production ambition to up to 10 GW by 2023, at least half of which would come from electricity hydrogen subject to affordability and value for money [4]. In addition, up to 20 GW of potential hydrogen projects have been identified in the UK pipeline through to 2037 [5], most of which select the renewables-powered electrolysis and the carbon capture, usage and storage (CCUS)-enabled methane reformation [6].

In order to achieve true carbon emission reductions, it is necessary to ensure electrolysis hydrogen production being powered by low carbon electricity generation such as fully dedicated renewables and otherwise curtailed renewable generation [6]. Furthermore, Green hydrogen produced from dedicated

renewables such as offshore wind not only ensures the low carbon nature of hydrogen production but will also allow hydrogen to act as an energy carrier for transporting and distributing renewable energy over long distances, especially when it is impractical or expensive to build or reinforce electricity grids [7]. For a 1.2 GW offshore wind farm requiring three to four 220 kV submarine cables for electricity delivery to shore, it was estimated that the supply and installation costs of hydrogen pipelines to shore were only around a third of those for laying submarine cables [8]. Given the need of 75 GW operating offshore wind capacity for the UK to reach net-zero carbon emissions in 2050 [9], the co-development of offshore wind and hydrogen can facilitate the integration of future high-level renewable energy into the energy systems. However, this poses many technical and commercial challenges [10] including but not limited to the integration of electrolysers (and fuel cells) within offshore wind farm infrastructures, the optimal system operation under varying offshore use case scenarios, and the ideal location/capacity of an offshore wind hydrogen system that can make the best business case for pilot and future projects.

To promote the investment into offshore wind hydrogen projects, the techno-economic simulation of an offshore wind and hydrogen co-location system for a specific offshore use case is required. This not only informs project developers of the techno-economics of the co-location project but can also be used in conjunction with an optimisation algorithm for the co-location project planning. Three system topologies have been investigated in [11] for offshore wind hydrogen production, including centralised electrolysis conducted onshore or at offshore central platforms and decentralised electrolysis placed at individual offshore wind turbines. Assuming the electrolyser capacity to be 80% of a 1.2 GW offshore wind farm that is 80 km from shore, the levelised costs of hydrogen (LCOH) produced by centralised onshore or offshore electrolysis were evaluated in [8] for 2020, 2030 and 2050 scenarios respectively; while the LCOH of the two topologies was forecast to reduce by almost 85% by 2030 and even further by 2050, the increased costs of installation, maintenance and operation for the offshore electrolysis led to a higher LCOH which, however, would reach comparable as the LCOH of the onshore electrolysis by 2050 [8]. For the decentralised offshore electrolysis, the ERM has implemented detailed bottom-up financial modelling of the first 10 MW Dolphyn commercial demonstrator that incorporates a polymer electrolyte membrane (PEM) electrolyser into a semi-submersible floating wind turbine, and estimated that a LCOH of around £1.5/kg would be available for bulk scale production from Dolphyn projects by 2040 [12]. In addition, the techno-economic overview and simulation of the three topologies along with varying electrolyser technologies and electricity/hydrogen co-generation modes were undertaken in [13] based on a reference case of 12 GW offshore wind hubs in North Sea. However, these research was mainly conducted by using a specific electrolyser capacity without optimisation.

The sizing problem of energy storage systems (ESSs) can be addressed by performing an economic optimisation subject to a set of technical constraints [14]. The optimal sizes of hydrogen-, ammonia- or battery-based ESSs co-located with a 1.5 GW hypothetical offshore wind farm were determined in [15] by maximising the net profit of the co-location system, i.e., the rise of the revenue from relevant energy markets above the investments into the ESSs. The operation of an offshore wind and hydrogen co-location system participating in the German electricity spot markets, ancillary service markets and the sale of hydrogen was designed in [16], based on which the hydrogen system was sized to either maximise the net present value or minimise the LCOH. The size and operation of an onshore hydrogen system co-located with offshore wind for the frequency response service provision were co-optimised in [17] to maximise the net present value of the co-location project based on the UK perspective. The offshore wind hydrogen system configuration for electricity market arbitrage or hydrogen production was designed separately in [18]; for each configuration, the operating strategies and hydrogen system capacities were determined to maximise the revenue and the return on investment in inner and outer optimisation layers respectively. Even though the sale of hydrogen has been considered a key revenue stream for offshore wind hydrogen systems, most research related to hydrogen system sizing problems did not take into account the local demand for hydrogen nor the diversity of offshore wind sources that might require coordinating the delivery of hydrogen from multiple hydrogen systems.

The contribution of this paper is to develop a modelling framework to optimise hydrogen system capacities for fully dedicated offshore wind hydrogen production systems which generate and store

hydrogen at offshore central platforms and transport hydrogen to shore via pipelines. In addition to reflecting the entire process of offshore wind hydrogen production and transportation, the modelling framework dispatches hydrogen from multiple systems to fulfil onshore demands and maintain similar state of charge (SOC) levels between their storage assets. The present values of hydrogen supply to various energy sectors are compared with the total present costs of offshore wind hydrogen systems in order to estimate their average LCOH at the end of a 20-year project lifespan. Then the particle swarm optimisation (PSO) algorithm is used to minimise the average LCOH by optimising hydrogen system capacities for a given wind farm scale. The effectiveness of the modelling framework is presented here through a case study at Milford Haven (South Wales) which will deliver a hydrogen-enabled multi-vector energy system to assist the UK in achieving net zero by 2050 [19]. The optimisation of offshore wind hydrogen production systems performed for 2030 and 2050 scenarios not only suggests the technology improvement required for developing feasible projects but can also help understand the potential level of green hydrogen supply to Milford Haven in the future.

The paper is structured as follows: Section 2 describes the estimation of offshore wind resources and hydrogen offtake options in the Milford Haven case study and the technical modelling of offshore wind hydrogen systems; Section 3 implements the PSO algorithm based on the techno-economic input parameters of the systems projected for 2030 and 2050 scenarios; Section 4 discusses the hydrogen system sizing results and the optimisation-based system operation and cost-benefit analysis; Section 5 presents conclusions and recommendations for further work.

## 2. Technical modelling of offshore wind hydrogen production system

### *2.1. Offshore wind resources in Celtic Sea*

Milford Haven will witness huge installed capacity of offshore renewable generation in the Celtic Sea, with five zones identified as more promising regions for floating offshore wind (FLOW) development, as shown in Figure 1(a) [20]. Zone 1 and Zone 5 closer to the coast of South Wales have a total area of about 10,283 $km^2$. Given a FLOW turbine deployment capacity of 3 or 4.8 $MW/km^2$ in the medium or high case respectively, the two zones might allow deploying multiple FLOW farms with total installed capacity ranging from around 31 to 49 GW. More than ten FLOW projects totalling around 2.2 GW have been planned in the Celtic Sea, with their approximate locations shown in Figure 1(b) [21]. The time-varying FLOW resources are evaluated here based on the MERRA-2 (Modern-Era Retrospective Analysis for Research and Applications, Version 2) reanalysis data of wind speeds which has a spatial resolution of $0.5^o$ latitude (~55 km) and $0.625^o$ longitude (~69 km) [22]. Considering that a maximum of 18.5 GW FLOW capacity could be deployed in a 3,800 $km^2$ MERRA square in the high case, two suitable MERRA squares following the planned FLOW projects are adopted here to approximate the regions of the future FLOW projects (see Figure 1(b)). The straight distances from the centres of the two squares, denoted by MERRA-S1 and MERRA-S2, to the onshore Pembroke substation at Milford Haven are about 122.5 and 150.6 km respectively. It is presumed here that 1,200 Vestas wind turbines V236-15.0 MW™ [23] are deployed in each square with 18 GW FLOW capacity in total. Then the hourly reanalysis data of wind speeds recorded for each square over 2016-2019 is converted into the time series of available FLOW power outputs by using a virtual wind farm model which considers the wind power smoothing effect across the square [24]. Figures 2(a) and 2(b) show the wind power curve for the 18 GW FLOW capacity and the resulting wind power data in each MERRA square respectively. The shift of wind power profiles in time between the two squares reflects the travel of wind from one square to another.

### *2.2. Hydrogen offtake options around Milford Haven*

The FLOW hydrogen production delivered to Milford Haven will not only be consumed locally within Pembrokeshire but can also be transported to neighbouring regions. Table 1 lists the timeline and daily hydrogen usage estimated for various hydrogen offtake options within Pembrokeshire or neighbouring regions. According to the purpose of hydrogen use, the offtake price of each option is determined here

by its break-even point at which the specific hydrogen use becomes cost competitive relative to a zero-carbon alternative [8]. Since the hydrogen production and storage might not always meet the required hydrogen demands, the priority of hydrogen supply is determined here based on the locations of the offtake options, followed by their break-even prices (see Table 1). In order to reflect the time-varying nature of hydrogen offtake, the (sub-) hourly hydrogen demands of power stations, vehicle hydrogen refuelling and marine vessels are synthesised here based on their daily usage in combination with final physical notifications (over 2016-2019), busy hours of petrol stations and time slots of vessel docking respectively. The daily hydrogen usage of the other offtake options is assumed to be evenly distributed across 24 hours. Figure 3(a) shows the profiles of aggregate hydrogen demands within Pembrokeshire and neighbouring regions synthesised over the four years. Assuming a hydrogen production efficiency of 22.2 kg/MWh, the total hydrogen production rates are calculated from FLOW power outputs in the two MERRA squares and compared with the total hydrogen demands, as shown in Figure 3(b). Their time-varying imbalances are induced by the intermittent nature of FLOW generation, highlighting the need of hydrogen storage assets for the time shift of hydrogen production.

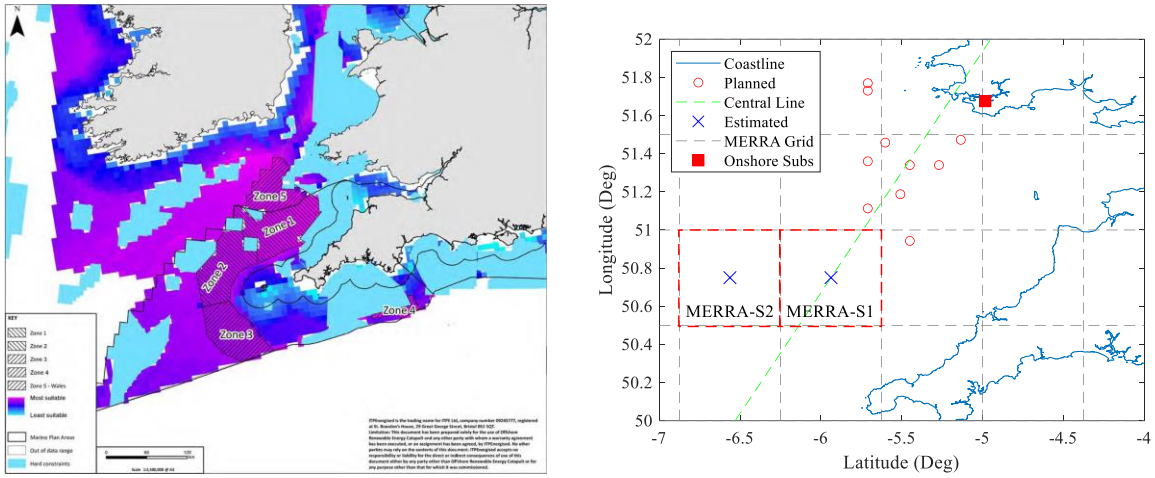


(a) (b)

**Figure 1.** Maps showing (a) five key zones identified for FLOW development and (b) planned FLOW projects and two MERRA squares selected for future FLOW development in the Celtic Sea.

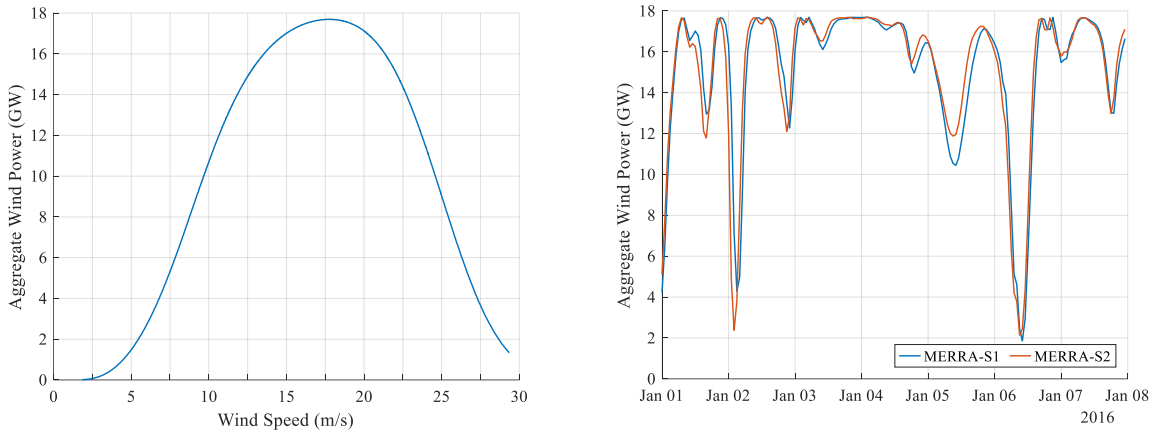


(a) (b)

**Figure 2**. (a) The power curve for 18 GW FLOW capacity and (b) the resulting wind power estimates (GW) over the first week of 2016 in each MERRA square.

**Table 1.** Hydrogen offtake options within Pembrokeshire or neighbouring regions and their estimated timeline, daily hydrogen usage, break-even prices, and offtake priority.

| Option | Purpose | Timeline | Usage (ton/day) | Price (£/kg) | Offtake Priority |
|---|---|---|---|---|---|
| Pembroke Oil Terminal | Bulk production & storage of liquid organic $H_2$ carrier or $NH_3$ for export | 2040 | 4,940.5 | 7.7 | 1 |
| Pembroke Refinery | Low carbon synthetic fuels | 2040 | 1,500.0 | 7.7 | 1 |
| Pembroke Dock | $H_2$ supply to marine vessels | 2035 | 17.1 | 3.5 | 3 |
| RWE Power Station | To fuel future $H_2$ gas turbines | 2040 | 1500.0 | 2.3 | 4 |
| Local Gas Network (Wales & West) | Potentially 100% into regional gas distribution system | 2032 | 45.0 | 2.2 | 5 |
| National Grid | Potentially inject to 100% $H_2$ backbone | 2030 | 250.0 | 2.2 | 5 |
| Pembroke Refinery | Industrial heat/grey $H_2$ replacement | 2030 | 200.0 | 1.5 | 7 |
| Milford Haven Port | Transport and heating requirements | 2030 | 2.5 | 1.5 | 7 |
| Pembroke Council | Vehicle fleet and $H_2$ refuelling hub | 2024 | 1.7 | 1.5 | 7 |
| Fishguard Dock | $H_2$ supply to marine vessels | 2035 | 5.2 | 3.5 | 10 |
| 520 MW Baglan Bay | To fuel future $H_2$ gas turbines | 2040 | 357.8 | 2.3 | 11 |
| 850 MW Severn Power | To fuel future $H_2$ gas turbines | 2040 | 584.9 | 2.3 | 11 |
| Tata Steel Port Talbot | $H_2$ requirement for steel production | 2030 | 721.4 | 1.8 | 13 |
| Celsa manufacturing | $H_2$ requirement for steel production | 2030 | 187.6 | 1.8 | 13 |
| Liberty Steel New | $H_2$ requirement for steel production | 2030 | 144.3 | 1.8 | 13 |
| Neighbouring Ports | Transport and heating requirement | 2030 | 0.6 | 1.5 | 16 |
| Neighbouring Councils | Vehicle fleet and $H_2$ refuelling hub | 2024 | 28.7 | 1.5 | 17 |

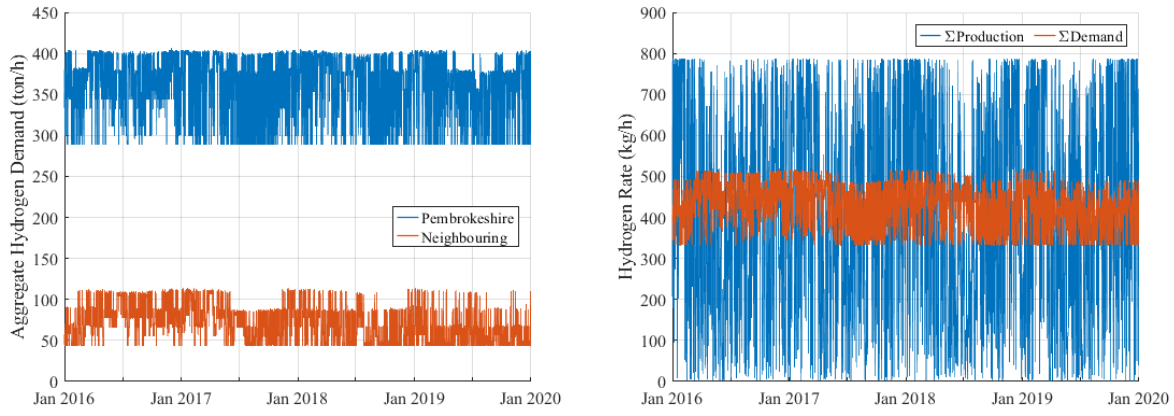


(a) (b)

**Figure 3**. (a) Time series (ton/hr) of aggregate hydrogen demands of Pembrokeshire and neighbouring regions and (b) their total demands against the total hydrogen production rates within the two MERRA squares synthesised based on historic data over 2016-2019.

### *2.3. Offshore wind hydrogen system modelling*

*2.3.1. Schematic.* Figure 4 shows the schematic of a centralised offshore wind hydrogen system where power outputs of FLOW turbines are collected by inter-array AC cables and transferred to an offshore central platform for green hydrogen production. Given the smoothing effect and intermittent nature of FLOW power outputs, an offshore central platform with an expected export capacity of no greater than 500 MW [25] is designed here to connect 40 Vestas 15 MW wind turbines, totalling 600 MW. This means that each MERRA square can comprise 30 offshore wind hydrogen systems which are assumed

to be configured and operated in the same way since the wind resource diversity across a single square is not modelled in this work. Since the layout optimisation of FLOW turbines and inter-array cables is outside the scope of this work, FLOW turbines are evenly distributed with a space $S_{WT}$ of 7 times the rotor diameter (i.e., ~2 km). Given the use of 630 mm$^2$, 81.7 MVA submarine AC cables, five 15 MW wind turbines are placed along each of the eight cable strings, forming a 600 MW wind turbine group. The power output of the 600 MW group delivered to the central platform is converted into DC power via an converter and then used by other hydrogen system components including a desalination device for seawater purification, an electrolyser for hydrogen production, and two compressors that pressurise hydrogen to reach the inlet pressure of 12 inch export pipeline or a higher pressure level for storage assets for later transportation to shore. In addition, a chemical storage device such as batteries requires to be deployed alongside the hydrogen system as backup power supply, though this is not modelled here for simplicity.

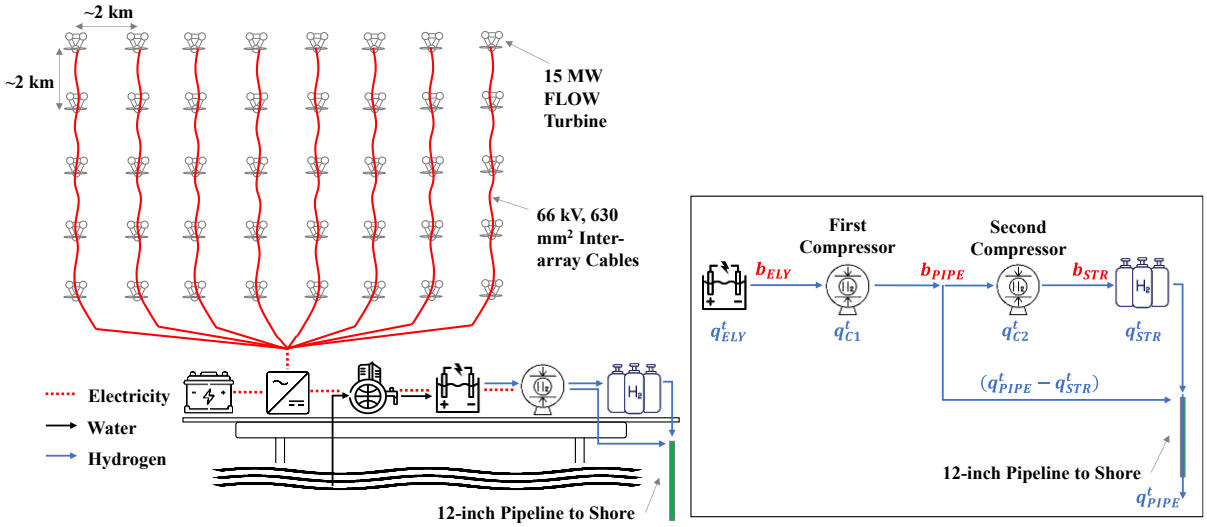


**Figure 4**. The schematic of a centralised offshore wind hydrogen system.

*2.3.2. Power flow balance.* Assuming that the FLOW turbines of each 600 MW group have the same outputs $P^t_{WT}$ (MW) at the time step $t$, the power delivered to the offshore central platform $P^t_{OCP}$ (MW) after cable losses is estimated by equation (1) subject to the AC/DC converter capacity $P^R_{CON}$:

$$P^t_{OCP} = \min\left(P^R_{CON},\ 40 \cdot P^t_{WT} - 8 \cdot \left((5 \cdot P^t_{WT}/66)^2 \cdot 2.3 + \sum_{i=1}^{4}(i \cdot P^t_{WT}/66)^2\right) \cdot S_{WT} \cdot r_{AC}\right) \quad (1)$$

where $r_{AC}$ denotes the AC resistance (Ω/km) of the 66 kV cable per unit length, and the distance from a cable string end to the central platform is assumed to be about 2.3 times the space $S_{WT}$ between wind turbines on average. After subtracting conversion losses, the remaining power is distributed among the desalination device $P^t_{DEL}$, electrolyser $P^t_{ELY}$, compressors $P^t_{C1}$ and $P^t_{C2}$:

$$P^t_{OCP} \cdot \eta_{CON} = P^t_{ELY} + P^t_{DEL} + P^t_{C1} + P^t_{C2} \quad (2)$$

where $\eta_{CON}$ is the efficiency of the converter, and

$$P^t_{ELY} = q^t_{ELY}/\eta^{P2H}_{ELY} \quad (3)$$

$$P^t_{DEL} = \eta_{DEL} \cdot q^t_{ELY}/\eta^{W2H}_{ELY} \quad (4)$$

$$P_{C1} = 10^{-6} \cdot \left(\frac{q^t_{C1}}{3600}\right) \cdot \frac{u \cdot Z_{C1} \cdot T}{M \cdot \eta_C} \cdot \frac{N_C \cdot \gamma}{\gamma - 1} \cdot \left(\left(\frac{b_{PIPE}}{b_{ELY}}\right)^{(\gamma-1)/(N_C \cdot \gamma)} - 1\right) \quad (5)$$

$$P_{C2} = 10^{-6} \cdot \left(\frac{q^t_{C2}}{3600}\right) \cdot \frac{u \cdot Z_{C2} \cdot T}{M \cdot \eta_C} \cdot \frac{N_C \cdot \gamma}{\gamma - 1} \cdot \left(\left(\frac{b_{STR}}{b_{PIPE}}\right)^{(\gamma-1)/(N_C \cdot \gamma)} - 1\right) \quad (6)$$

where $q_{ELY}^t$ (kg/h), $\eta_{ELY}^{P2H}$ (kg/MWh) and $\eta_{ELY}^{W2H}$ (kg/L) denote the hydrogen production rate, power- and water-to-hydrogen efficiencies of the electrolyser respectively; $\eta_{DEL}$ (MWh/L) is the power usage of the desalination device per unit of seawater purified; $q_{C1}^t$ or $q_{C2}^t$ (kg/h) is the hydrogen flow rate of the first compressor that pressurises hydrogen from the production pressure $b_{ELY}$ (bar) to the inlet pressure of the pipeline $b_{PIPE}$ (bar) and the second compressor that further pressurises hydrogen to the pressure for storage $b_{STR}$ (bar); $u$ is the universal constant of ideal gas equalling 8.314 J/mol-K; terms $T$, $M$ and $\gamma$ are the temperature, molecular mass and heat capacity ratio of hydrogen that equal 288.15 K, 2.15 x $10^{-3}$ kg/mol and 1.41 respectively; $Z_{C1}$ and $Z_{C2}$ are the hydrogen compressibility factors determined by $T$ and associated compressor pressure levels; and the two compressors are presumed to have the same efficiency $\eta_C$ of 75% and a single compression stage ($N_C = 1$) [26]. In addition, the degradation of the electrolyser stacks with operating time is simulated here by linearly reducing the efficiencies $\eta_{ELY}^{P2H}$ and $\eta_{ELY}^{W2H}$ from their respective nominal levels to 90% of the nominal levels at the end of the stack lifetime [17]; then the electrolyser will be replaced to restore $\eta_{ELY}^{P2H}$ and $\eta_{ELY}^{W2H}$ to the nominal levels.

*2.3.3. Hydrogen flow balance*. Equation (7) depicts the hydrogen flow balance within the hydrogen system that delivers $q_{PIPE}^t$ to shore via the 12 inch pipeline (see Figure 4). The rate of hydrogen injected into the storage $q_{C2}^t$ or released from the storage $q_{STR}^t$ is determined by the difference between $q_{PIPE}^t$ and $q_{C1}^t$. The resulting hydrogen storage level $Q_{STR}^t$ (kg) is updated by equation (8) where $\Delta t$ (h) is the time step length in the simulation.

$$q_{ELY}^t = q_{C1}^t = q_{PIPE}^t + q_{C2}^t - q_{STR}^t = q_{PIPE}^t + \min(q_{C1}^t - q_{PIPE}^t, 0) - \min(q_{PIPE}^t - q_{C1}^t, 0) \quad (7)$$

$$Q_{STR}^t = Q_{STR}^{t-1} + (q_{C2}^t - q_{STR}^t) \cdot \Delta t \quad (8)$$

*2.3.4. Hydrogen dispatch.* The hydrogen delivery from the offshore wind hydrogen systems in the two MERRA squares is dispatched to meet the total onshore hydrogen demands subject to the availability of hydrogen production and storage. Specifically, the supply $q_{PIPE}^t$ of the system is first contributed by the direct hydrogen production, followed by the hydrogen discharge from the storage. Furthermore, to maintain similar SOC levels between multiple systems, the systems having higher relative availability (i.e., the sum of hydrogen production $q_{ELY}^t \cdot \Delta t$ and present hydrogen storage $Q_{STR}^{t-1}$ in percentage of the storage capacity) are first used for hydrogen supply until the onshore demand is fully provided or their relative availability declines to the level of other systems; if the onshore hydrogen demand is not fully met, then the remaining demand requirement will be split among all the systems in proportion to their storage capacities. In addition, the hydrogen delivery to shore is limited by the capacity of the 12 inch pipeline that is determined by its diameter and acceptable operational velocity. The latter is dominated by the outlet pressure of the pipeline [27] which is set to 68 bar in this work to facilitate the integration with onshore gas network. When the hydrogen transportation to shore is constrained, the systems with headroom in pipeline capacity will be used to fill in the shortage of hydrogen supply regardless of the resulting differences in SOC levels between systems.

## 3. Techno-economic optimisation of offshore wind hydrogen system

### *3.1. Optimisation variables*

Since the offshore wind hydrogen systems experiencing the same wind resources in a MERRA square are configured and operated in the same way, the optimsiation of a representative system is applicable to the other 29 systems within the same square. The optimsiation variables specified here comprise the electrolyser capacity of the representative system in each square, the storage capacity of the system in MERRA-S1 and the capacity ratio $r_C$ between the two compressors, as shown in Figure 5, which are used to size all the hydrogen system components based on their capacity dependencies described by equations (2)-(6). Furthermore, it is assumed here that the storage asset capacity is proportional to the electrolyser capacity and the central platform size (in MW) is determined by the converter capacity.

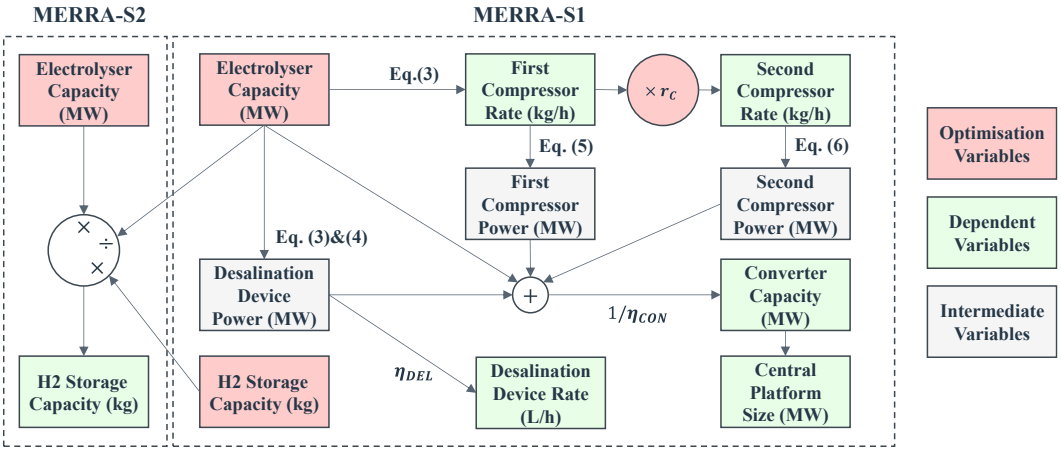


**Figure 5.** The hydrogen system components that are directly or indirectly optimised.

### *3.2. PSO implementation*

The optimisation variables specified in Figure 5 are estimated here by the PSO algorithm [28], aiming to minimise the average LCOH of offshore wind hydrogen systems in the two MERRA squares given an annual return of 8%:

$$LCOH = \left(CAPEX_{FLOW} + CAPEX_{HYS} + \sum_{m=1}^{240} \frac{OPEX_{FLOW}^{m} + OPEX_{HYS}^{m} + REPEX_{PEM}^{m}}{(1+8\%)^{m/12}}\right) \Big/ \sum_{m=1}^{240} \frac{Q_{PIPE}^{m}}{(1+8\%)^{m/12}} \quad (9)$$

where $m$ is the month index starting from 1 to 240 (i.e., 20 years); $CAPEX_{FLOW}$ and $CAPEX_{HYS}$ are the overall capital expenditures of FLOW farms and hydrogen systems respectively; $OPEX_{FLOW}^{m}$ and $OPEX_{HYS}^{m}$ are the monthly operating expenses of FLOW farms and hydrogen systems; $REPEX_{PEM}^{m}$ is the replacement expenditure of PEM electrolysers occurring in the month $m$; and $Q_{PIPE}^{m}$ represents the total hydrogen demand (kg) supplied in the month $m$. The PSO process will be implemented here by using the techno-economic parameters of semi-submersible FLOW farms and PEM-based hydrogen systems projected for 2030 and 2050 respectively, as listed in in Table 2, in order to assess the impacts of techno-economic improvement on the optimisation results. It is noted that the economics estimated by the references for past years or different currency units have been converted to 2019 values in GBP (British Pound Sterling).

## 4. Optimisation and simulation results

The techno-economic simulation of offshore wind hydrogen systems and the PSO implementation are accomplished here using MATLAB/Simulink [37]. This section first discusses the hydrogen system sizing results obtained based on the techno-economic input parameters for 2030 and 2050, followed by presenting the optimisation-based system operation and cost-benefit analysis to illustrate the model effectiveness and the prospect of offshore wind hydrogen projects in the Milford Haven case study.

### *4.1. Optimisation results*

The optimal capacities of the hydrogen system components co-located with a representative 600 MW FLOW farm in each MERRA square are tabulated in Table 3. The optimisation results are very similar between the two squares, though the hydrogen systems in MERRA-S2 have greater capacities than those in MERRA-S1 due to the higher load factor of FLOW farms in MERRA-S2. With further improvements in hydrogen technologies in 2050, the hydrogen systems optimised with higher nominal production rates require larger capacities of desalination devices and compressors along with greater storage capacities so as to deliver more hydrogen to shore. However, the electrolyser capacity which dominates the capacities of converter and offshore central platform is reduced in the 2050 scenario due to the increased electrolyser efficiency. It is evaluated that the best electrolyser capacities are around 71%-72% and 67%-68% of the FLOW capacity in 2030 and 2050 scenarios respectively.

**Table 2.** Techno-economic parameters of offshore wind hydrogen systems in 2030 and 2050 scenarios.

| Component | Variable | Unit | 2030 | 2050 | Ref. |
|---|---|---|---|---|---|
| Semi-submersible FLOW Turbines & Platform | Unit CAPEX | £/MW | 2204.4 | 1764.2 | [29], [30] |
| | Unit OPEX | £/MW/yr | 55.1 | 44.1 | [29], [30] |
| 66 kV, 630 mm$^2$ Inter-array AC Cable | AC Resistance | Ω/km | 0.0274 | 0.0274 | [31] |
| | Unit CAPEX | £/m | 398.6 | 398.6 | [31] |
| | Unit OPEX | £/m/yr | 12.0 | 12.0 | [31] |
| Offshore Central Platform | Unit CAPEX | £/MW | 264.0 | 264.0 | [8] |
| | Unit OPEX | £/MW/yr | 2.9 | 2.9 | [8] |
| AC/DC Converter | $\eta_{CON}$ | % | 95.0 | 95.0 | [17] |
| | Unit CAPEX | £/MW | 75.0 | 75.0 | [17] |
| | Unit OPEX | £/MW/yr | 1.5 | 1.5 | [17] |
| Reverse Osmosis Desalination Device | $\eta_{DEL}$ | MWh/L | 5 x $10^{-6}$ | 5 x $10^{-6}$ | [32] |
| | Unit CAPEX | £/(L/h) | 32.1 | 20.5 | [33] |
| | Unit OPEX | £/(L/h)/yr | 1.0 | 1.0 | [13] |
| PEM Electrolyser | $\eta_{ELY}^{P2H}$ | kg/MWh | 20.4 | 22.2 | [34] |
| | $\eta_{ELY}^{W2H}$ | kg/L | 0.0756 | 0.0822 | [34] |
| | $b_{ELY}$ | bar | 50 | 70 | [34] |
| | Stack Lifetime | OP Hours | 90,000 | 120,000 | [34] |
| | Unit CAPEX | £/MW | 838.5 | 429.0 | [34] |
| | Unit OPEX | £/MW/yr | 16.8 | 8.6 | [34] |
| | Unit REPEX | £/MW | 251.6 | 128.7 | [35] |
| 50 kg/hr, 30 bar-200 bar Reference Compressor [a] | Unit CAPEX | £ | 281,388.6 | 281,388.6 | [35] |
| | Unit OPEX | £/yr | 11,255.5 | 11,255.5 | [13] |
| Hydrogen Storage Tank | $b_{STR}$ | bar | 350 | 350 | [35] |
| | Unit CAPEX | £/kg | 440.8 | 440.8 | [35] |
| | Unit OPEX | £/kg/yr | 8.8 | 8.8 | [35] |
| 12 Inch Hydrogen Pipeline | $b_{PIPE}$ | bar | 73~75 acc. pressure drop | | [27] |
| | Unit CAPEX | £/m | 267.6 | 267.6 | [36] |
| | Unit OPEX | £/m/yr | 8.0 | 8.0 | [36] |
| System Integration Test | Unit CAPEX | £/site | 10,263.8 | 10,263.8 | [36] |

[a] Please refer to [17] for the cost calculation of compressors based on a reference compressor system.

**Table 3.** The hydrogen system capacities optimised for a representative 600 MW FLOW farm in each MERRA square based on techno-economic input parameters in 2030 and 2050 scenarios.

| Hydrogen System Component | MERRA Square | 2030 | 2050 |
|---|---|---|---|
| PEM Electrolyser (MW) | MERRA-S1 | 426.1 | 405.4 |
| | MERRA-S2 | 429.6 | 408.1 |
| Desalination Device (L/h) | MERRA-S1 | 130,388.6 | 135,001.7 |
| | MERRA-S2 | 131,459.9 | 135,880.5 |
| First Compressor (kg/h) | MERRA-S1 | 8,692.6 | 9,000.1 |
| | MERRA-S2 | 8,764.0 | 9,058.7 |
| Second Compressor (kg/h) | MERRA-S1 | 2,792.7 | 2,984.7 |
| | MERRA-S2 | 2,815.7 | 3,004.2 |
| Converter (MW) | MERRA-S1 | 451.7 | 430.2 |
| | MERRA-S2 | 455.5 | 433.0 |
| Storage Asset (kg) | MERRA-S1 | 97,882.4 | 102,670.7 |
| | MERRA-S2 | 98,686.7 | 103,339.1 |

### *4.2. Optimisation-based system operation*

Figure 6(a) shows the aggregate available power output of a 600 MW FLOW farm in MERRA-S1, the power available at the central platform after slight inter-array cable losses, the power available for the hydrogen system subject to the conversion capacity and efficiency, and the power eventually absorbed by the electrolyser, desalination device and compressors during a particular simulation day in 2050 scenario. The hydrogen flow rates and resulting SOC levels of a single storage asset and the overall hydrogen supply of the systems in each square over the same day are shown in Figure 6(b) and 7(a) respectively. In the first six hours of the day, the hydrogen systems consume only part of the available power (see Figure 6(a)) for hydrogen production which fully meets onshore demands (see Figure 7(a)), keeping SOC levels at 100% (see Figure 6(b)). When the available FLOW generation decreases over 126-134 h, the hydrogen produced from the remaining power (after losses in cables and converters, see Figure 6(a)) meets only part of onshore demands, which requires additional supply from storage assets and reduces their SOC levels, as shown in Figures 7(a) and 6(b). When it comes back to the high wind period over 134-144 h, the power available for the hydrogen system is fully used to produce hydrogen (see Figure 6(a)), part of which is transported to shore (see Figure 7(a)) while the other part is pressurised further through the second compressor and stored in storage assets (see Figure 6(b)). In addition, Figure 6(b) shows that the SOC levels of the systems in the two MERRA squares are almost the same, illustrating the effectiveness of the specific hydrogen dispatch strategy designed in this work. The distribution of hydrogen supply across different offtake options during the same day is shown in Figure 7(b) where all the hydrogen demands are met, though the options having higher offtake priority form the base of the hydrogen supply.

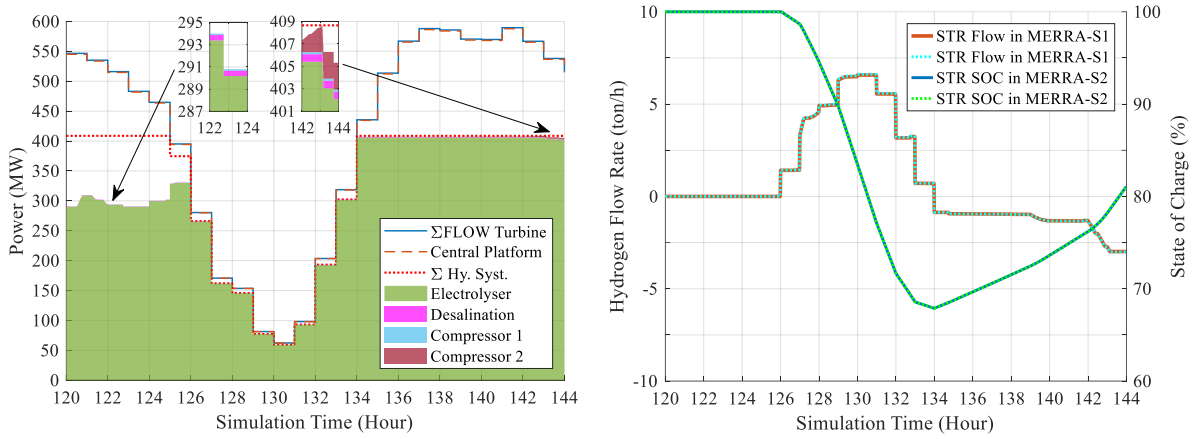


(a) (b)

**Figure 6**. (a) The power (MW) available at the FLOW farm, central platform and hydrogen system and absorbed by the electrolyser, desalination and compressors of a 600 MW system in MERRA-S1, and (b) the hydrogen flow rates (ton/h) and SOC levels (%) of a single storage asset in MERRA-S1 or MERRA-S2 during a particular simulation day over 120-144 h.

### *4.3. Cost-benefit analysis and hydrogen supply*

The cumulative present revenue and costs of the representative offshore wind hydrogen system in each MERRA square are shown in Figure 8(a) respectively. The total system costs mainly come from the CAPEX of FLOW turbines, PEM electrolyser and central platform, followed by the overall OPEX of the FLOW farm and the hydrogen system. Furthermore, the REPEX of electrolyser stacks occurring at the 11$^{th}$ (or 14$^{th}$) year in the 2030 (or 2050) scenario contributes only a small part to the total system costs. Although greater hydrogen production capabilities are used to supply more hydrogen to shore in the 2050 scenario (see Figure 8(b)), the total system costs are largely reduced in the 2050 scenario due to the price drops of wind turbines, electrolysers, etc. The decreases of total system costs together with the growths of hydrogen supply not only lead to the LCOH reduction, but also increase the net present

value of the system. It is evaluated that the LCOH and net present value of the representative system in MERRA-S1 (or MERRA-S2) are around £5.35/kg and £0.29bn (or £5.32/kg and £0.31bn) in the 2030 scenario, or £3.88/kg and £1bn (or £3.87/kg and £1.02bn) in the 2050 scenario respectively.

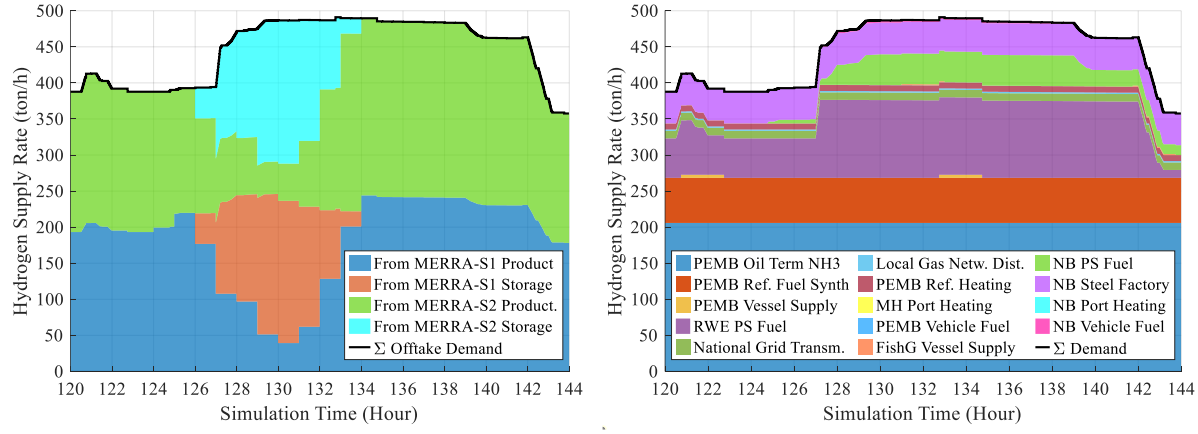


(a) (b)

**Figure 7.** (a) The overall hydrogen supply rates (ton/h) by direct production and storage release in the two MERRA squares, and (b) the distribution of hydrogen supply (ton/h) across offtake options during a particular simulation day over 120-144 h.

As shown in Figure 8(b), the annual hydrogen demand of the offtake options within Pembrokeshire and neighbouring regions is evaluated to be around 3.84 million tons in total, 73% or 76.6% of which would be met on average by the systems in the two squares in the 2030 or 2050 scenario respectively. Most of the hydrogen production is shown to be used by Pembroke Oil Terminal for $NH_3$ production, Pembroke Refinery for low-carbon fuel synthesis, and RWE power station due to their higher offtake priority and large demands for hydrogen. Figure 9 shows the percentage of the annual demand of each offtake option that would be supplied by the FLOW hydrogen production in the 2030 or 2050 scenario, which generally declines with the decreasing offtake priority. The systems in the two MERRA squares would supply about 85%-90% of the demand of the highest-priority Pembroke Oil Terminal and 55%-75% of the demands for most of the other offtake options.

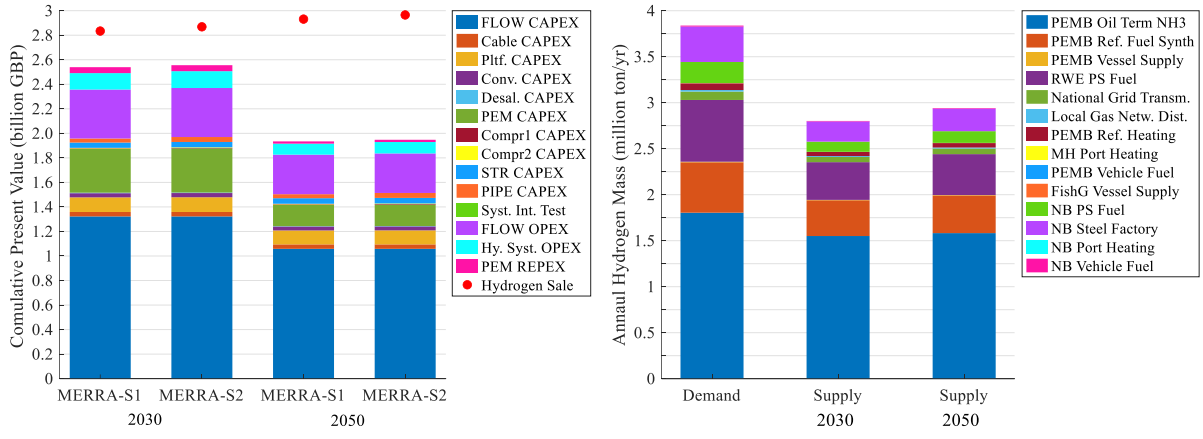


(a) (b)

**Figure 8.** (a) Cumulative present values (billion GBP) of hydrogen sale and costs of the representative offshore wind hydrogen system in each MERRA square, and (b) the annual hydrogen demands (ton/yr) supplied by the systems to different offtake options on average in 2030 and 2050 scenarios.

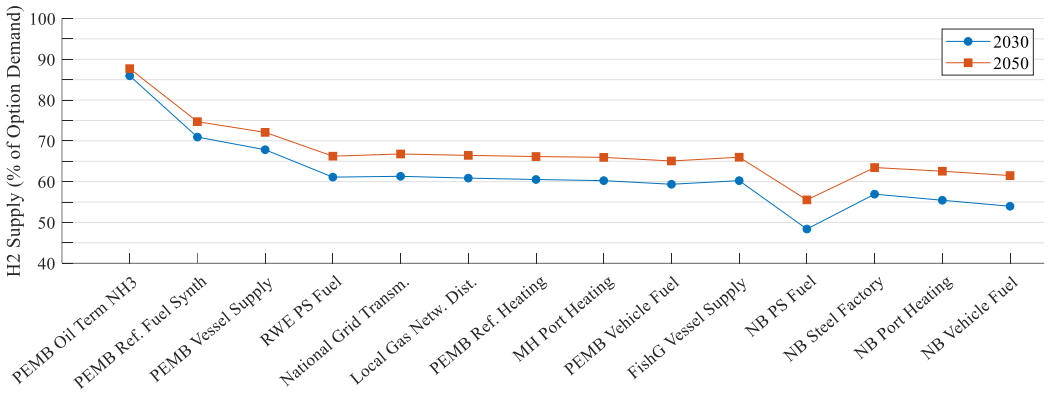


**Figure 9.** The percentages of hydrogen demands of different offtake options met by the offshore wind hydrogen systems in the two MERRA squares in 2030 and 2050 scenarios.

## 5. Conclusion and future work

With the development of electrolyser technologies, dedicated offshore wind farms for green hydrogen production is considered a cost-effective approach to exploiting deep offshore wind resources which can be carried to different energy sectors in the form of hydrogen. To facilitate the co-development of offshore wind and hydrogen systems, this paper has proposed a modelling framework to optimise the capacities of the centralised hydrogen systems that are co-located with offshore wind farms to produce, pressurise, store and transport hydrogen to shore. The power transfer from floating wind turbines to an offshore central platform and the power distribution among hydrogen system components have been simulated by considering the losses in power transmission and conversion and the dependent operation of hydrogen system components respectively. Furthermore, the hydrogen production and storage of multiple systems have been dispatched to meet onshore demands while keeping similar state of charge levels between systems, based on which the hydrogen system power consumptions were determined subject to their own power capacities and available wind power outputs. Then the present values of the hydrogen supply and total system costs were translated into the levelised cost of hydrogen (LCOH) of the system, which was minimised by the particle swarm optimsiation algorithm to estimate the optimal hydrogen system capacities. The proposed modelling framework has been validated in the context of Milford Haven in South Wales, with the associated hydrogen demands and offshore wind resources available for hydrogen production being estimated. The techno-economic parameters of the system components (e.g., semi-submersible wind turbines and polymer electrolyte membrane electrolysers) projected for 2030 and 2050 scenarios have been used in the optimisation process separately to assess the effects of techno-economic improvements in relevant technologies on the hydrogen system sizing.

For an offshore wind hydrogen system comprising 600 MW wind turbines, it has been suggested to deploy an electrolyser with capacity equalling 71%-72% or 67%-68% of the wind farm capacity in the 2030 or 2050 scenario respectively. Although the electrolyser size was reduced in the 2050 scenario, the system achieved a higher nominal hydrogen production rate due to the improvement in electrolyser efficiency. The higher production rate has increased the sizes of desalination devices and compressors and required greater storage capability to deal with the imbalance between hydrogen production and demands. With the system component prices falling in the 2050 scenario, the offshore wind hydrogen systems with greater production capacities would cost less than those in the 2030 scenario. The system cost reduction together with the growth of hydrogen supply resulted in a LCOH of around £3.9/kg in the 2050 scenario which was smaller than the LCOH of around £5.3/kg in the 2030 scenario. Given 60 offshore wind hydrogen systems being installed (i.e., 36 GW wind power capacity in total), their total hydrogen supply would meet about 73% or 76.6% of onshore demands (i.e., totaling 3.84 million tons per year) in the 2030 or 2050 scenario respectively.

The proposed modelling framework will be further developed to not only incorporate the objective function of net present value maximisation, but also enable the optimisation of decentralised offshore

wind hydrogen systems. This will assist in understanding the effects of objective functions and system configurations on the hydrogen system optimisation. Furthermore, the hydrogen pipeline diameter will be modelled as an additional optimisation variable. Future work will also simulate wind resources at a higher spatial resolution. The increased diversity of wind resources across wind turbines will incur in the need of a more complicated strategy for hydrogen dispatch between multiple systems.

**Acknowledgments**
This work was conducted as part of the research programme of the Electrical Infrastructure Research Hub in collaboration with the Offshore Renewable Energy Catapult.

**References**
[1] HM Government 2020 *The Ten Point Plan for a Green Industrial Revolution* (London UK)
[2] International Renewable Energy Agency 2019 *Hydrogen: A Renewable Energy Respective* (Abu Dhabi United Arab Emirates)
[3] HM Government 2021 *UK Hydrogen Strategy* (London UK)
[4] Department for Business, Energy and Industrial Strategy 2022 *British Energy Security Strategy* (London UK)
[5] Department for International Trade 2022 *Hydrogen Invstor Roadmap – Leading the Way to Net Zero* (London UK)
[6] HM Government 2022 *Hydrogen Strategy Update to the Market: July 2022* (London UK)
[7] International Renewable Energy Agency 2018 *Hydrogen from Renewable Power – Technology Outlook for the Energy Transition* (Abu Dhabi United Arab Emirates)
[8] Spyroudi A, Wallace D, Smart G, Stefaniak K, Mann S and Kurban Z 2020 *Offshore Wind and Hydrogen – Solving the Integration Challenge* (Glasgow UK: Offshore Renewable Energy Catapult)
[9] Committee on Climate Change 2019 *Net Zero: The UK's Contribution to Stopping Global Warming* (London UK)
[10] Wu Y, Liu F, Wu J, He J, Xu M and Zhou J 2022 Barrier identification and analysis framework to the development of offshore wind-to-hydrogen projects *Energy* **239 B** 122077
[11] Ibrahim O S, Singlitico A, Proskovics R, McDonagh S, Desmond C and Murphy J D 2022 Dedicated large-scale floating offshore wind to hydrogen: Assessing design variables in proposed typologies *Renewable Sustainable Energy Rev.* **160** 112310
[12] Caine D, Wahyuni W, Pizii B, Iliffe M, Whitlock Z, Ryan B and Bond L 2021 *ERM Dolphyn Hydorgen: Phase 2 – Final Report* (Manchester UK: ERM)
[13] Singlitico A, Østergaard J and Chatzivasileiadis 2021 Onshore, offshoe or in-turbine electrolysis? Techno-economic overivew of alternative integration designs for green hydrogen production into offshore wind power hubs *Renewable Sustainable Energy Transition* **1** 100005
[14] Fan F, Zorzi G, Campos-Gaona D and Nwobu J 2022 Wind-plus-battery system optimisation for frequency resposne service: the UK perspective *Electr. Power Syst. Res.* **211** 108300
[15] Baldi F, Coraddu A, Kaliktzarakis M, Jeleňová D, Collu M, Race J and Maréchal F 2022 Optimisation-based system designs for deep offshore wind farms including power to gas technologies *Appl. Energy* **310** 118540
[16] Scolaro M and Kittner N 2022 Optimizing hybrid offshore wind farms for cost-competitive hydrogen production in Germany *Int. J. Hydrogen Energy* **47** 6478-93
[17] Fan F, Skellern S, Campos-Gaona D and Nwobu J 2023 Wind farm and hydrogen storage co-location system optimisation for dynamic frequency response in the UK *Clean Energy*
[18] Hóu P, Enevoldsen P, Eichman J, Hu W, Jacobson M Z and Chen Z 2017 Optimizing investments in coupled offshore wind-electrolytic hydrogen storage systems in Denmark *J. Power Sources* **359** 186-97
[19] Mee D, Elks S, Szczepanski M, Ageyman-Buahin P and Bridge F 2021 *Milford Haven: Energy Kingdom – System Architecture Report* (Birmingham UK: Energy Systems Catapult)

[20] Knight M, Smith L, Bawn G and Gibson T 2020 *Floating Offshore Wind Constraint Mapping in the Celtic Sea* (Glasgow UK: Offshore Renewable Energy Catapult)
[21] 4C Offshore 2023 *Global Offshore Renewable Map* (Lowestoft UK)
[22] Gelaro R, McCarty W, Suárez M J, Todling R, Molod A, Takacs L, et al 2017 The Modern-Era Retrospective Analysis for Research and Applications, Version 2 (MERRA-2) *J. Climate* **30** (14) 5419-54
[23] Vestas 2023 *V236-15.0 MW™* (Aarhus Denmark)
[24] Staffell I and Pfenninger S 2016 Using bias-corrected reanalysis to simulate current and future wind power output *Energy* **114** 1224-39
[25] Robak S and Raczkowski R M 2018 Substations of offshore wind farms: a review from the perspective of the needs of the Polish wind energy sector *Bulletin Polish Academy Sci. Tech. Sci.* **66** (4) 517-28
[26] Nexant, Inc. 2008 *H2A Hydorgen Delivery Infrastructure Analysis Models and Conventional Pathway Options Analysis Results* (Colorado USA)
[27] Menon E S 2011 *Pipeline Planning and Construction Field Manual* (Oxford UK: Gulf Professional Publishing, Elsevier Inc.)
[28] Kennedy J and Eberhar R 1995 Partile swarm optimization. *Proc. ICNN'95 – Int. Conf. Neural Networks* **4** 1942-48
[29] Stehly T, Beiter P and Duffy P 2020 *2019 Cost of Wind Energy Review* (Colorado USA: National Renewable Energy Laboratory)
[30] National Renewable Energy Laboraty 2022 *Annual Technology Baseline* (Colorado USA)
[31] TenneT 2015 *66 kV Systems for Offshore Wind Farms* (Arnhem Netherlands)
[32] Baldinelli A, Barelli L, Bidini G, Cinti G, Di Michele A and Mondi F 2020 How to power the energy-water nexus: coupling desalination and hydrogen energy storage in mini-grids with reversible solid oxide cells *Processes* **8** (11) 1494
[33] Caldera U and Breyer C 2017 Learning curve for seawater reverse osmosis desalination plants: capital cost trend of the past, present, and future *Water Resources Research* **53** (10) 523-38
[34] International Energy Agency 2019 *The Future of Hydrogen* (Paris France)
[35] Fuel Cells and Hydrogen 2 Joint Undertaking 2017 *Study on Early Business Cases for $H_2$ in Energy Storage and More Broadly Power to $H_2$ Applications* (Brussels Belgium)
[36] Bai Y and Bai Qiang 2010 Chapter 6 Subsea cost estimation *Subsea Engineering Handbook* 159-92 (Massachusetts USA: Gulf Professional Publishing)
[37] The MathWorks Inc. 2018 *MATLAB Release 2018b* (Massachusetts USA)